Theor Chem Account (2008) 120:351–361
DOI 10.1007/s00214-008-0435-6

REGULAR ARTICLE

Analysis of the metal–ligand bonds in $[Mo(X)(NH_2)_3]$ (X = P, N, PO, and NO), $[Mo(CO)_5(NO)]^+$, and $[Mo(CO)_5(PO)]^+$

Giovanni F. Caramori · Gernot Frenking

Received: 12 November 2007 / Accepted: 25 February 2008 / Published online: 12 March 2008

Abstract Quantum chemical calculations at the DFT level have been carried out for model complexes $[Mo(P)(NH_2)_3]$ (**1**), $[Mo(N)(NH_2)_3]$ (**2**), $[Mo(PO)(NH_2)_3]$ (**3**), $[Mo(NO)(NH_2)_3]$ (**4**), $[Mo(CO)_5(PO)]^+$ (**5**), and $[Mo(CO)_5(NO)]^+$ (**6**). The equilibrium geometries and the vibration frequencies are in good agreement with experimental and previous theoretical results. The nature of the Mo–PO, Mo–NO, Mo–PO^+, Mo–NO^+, Mo–P, and Mo–N bond has been investigated by means of the AIM, NBO and EDA methods. The NBO and EDA data complement each other in the interpretation of the interatomic interactions while the numerical AIM results must be interpreted with caution. The terminal Mo–P and Mo–N bonds in **1** and **2** are clearly electron-sharing triple bonds. The terminal Mo–PO and Mo–NO bonds in **3** and **4** have also three bonding contributions from a σ and a degenerate π orbital where the σ components are more polarized toward the ligand end and the π orbitals are more polarized toward the metal end than in **1** and **2**. The EDA calculations show that the π bonding contributions to the Mo–PO and Mo–NO bonds in **3** and **4** are much more important than the σ contributions while σ and π bonding have nearly equal strength in the terminal Mo–P and Mo–N bonds in **1** and **2**. The total $(NH_2)_3$Mo–PO binding interactions are stronger than for $(NH_2)_3$Mo–P which is in agreement with the shorter Mo–PO bond. The calculated bond orders suggest that there are only $(NH_2)_3$ Mo–PO and $(NH_2)_3$Mo–NO double bonds which comes from the larger polarization of the σ and π contributions but a closer inspection of the bonding shows that these bonds should also be considered as electron-sharing triple bonds. The bonding situation in the positively charged complexes $[(CO)_5Mo–(PO)]^+$ and $[(CO)_5Mo–(NO)]^+$ is best described in terms of $(CO)_5Mo \rightarrow XO^+$ donation and $(CO)_5Mo \leftarrow XO^+$ backdonation (X = P, N) using the Dewar–Chatt–Duncanson model. The latter bonds are stronger and have a larger π character than the Mo-CO bonds.

Keywords Nitric oxide · Phosphorus oxide · Molybdenum complexes · Energy decomposition analysis · AIM · NBO

1 Introduction

Phosphorus monoxide is a spectroscopically well-characterized molecule [1–9] and it is one of the most abundant phosphorus-containing compounds in interstellar space [10–12]. However, the coordination chemistry of PO is much less developed [13–21] in comparison with its analogue NO [22–28], due mainly to the intrinsic instability of PO in relation to the oxides P_4O_6 and P_4O_{10} [29,30]. Therefore, the coordination chemistry of PO represents a real challenge to inorganic chemists.

Due to the pioneering work of Scherer and co-workers [31] the first metal complexes bearing PO as a ligand have been synthesized and the structure could become characterized by X-ray structure analysis. They performed an oxidative cleavage of P–P bond of $(\eta^5 - C_5HPr^i_4)_2Ni_2W(CO)_4P_2$

Contribution to the Nino Russo 60th Birthday Festschrift Issue.

Theoretical Studies of Inorganic Compounds. 39. Part 38: A. Krapp, M. Lein, G. Frenking, Theoret. Chem. Acc., ASAP.

Electronic supplementary material The online version of this article (doi:10.1007/s00214-008-0435-6) contains supplementary material, which is available to authorized users.

G. F. Caramori · G. Frenking (✉)
Fachbereich Chemie, Philipps-Universität,
Hans-Meerwein-Strasse, 35032 Marburg, Germany
e-mail: frenking@chemie.uni-marburg.de

G. F. Caramori
e-mail: caramori@chemie.uni-marburg.de

complex with bis-trimethylsilyl peroxide, obtaining the analogous ($\eta^5 - C_5HPr^i_4$)$2Ni_2W(CO)_4(PO)_2$, in which the PO groups assume μ_3-coordination. The authors reported that the PO bond lengths (1.462 – 1.480 Å) showed good agreement with calculated [32–34] and experimental values [33] for isolated PO molecule, while the stretching frequency of PO ($\nu = 1{,}260\,cm^{-1}$) was slightly larger than for free PO ($\nu = 1{,}218\,cm^{-1}$) and P_4O($\nu = 1{,}240\,cm^{-1}$) [31,35].

In later experimental studies, different strategies for accessing PO complexes have been proposed [16–21]. For instance, the hydrolytic cleavage of PN bonds in aminophosphinidene ($\mu_3 - PNR_2$) and ($\mu_4 - PNR_2$) clusters [16,17,19,20], and the transference of oxygen atom to phosphide terminal complexes [36,37] through dimethyldioxirane oxidation [18], allowed the preparation of various complexes containing PO as ligand for different transition metals such as Ru, Co, Os, W, and Mo [16–21].

The nature of the chemical bonding between transition metals and PO has been a topic of debate in experimental and theoretical chemistry [16–25,27,28,38]. Comparisons between TM–NO and TM–PO reveal particular features of the TM-PO bond. The PO stretching frequency in TM-PO is in most cases below that of free PO. However, for some complexes such as [$\eta^5 - C_5H_5(CO_2)Mo]_3PO$, [$\eta^5 - C_5H_5(CO_2)Mo]_3PO$, and (OP)Mo[N(R)Ar]$_3$, ν(PO) is slightly above that of free PO [15,39]. Only few theoretical studies have been devoted to investigate the nature of the TM–PO bond in molybdenum and ruthenium complexes [38] or to gain insight into the nature of TM≡P and TM–PS bonds in some molybdenum and tungsten–phosphorus complexes [40]. Bérces and co-workers [38] presented a study about the nature of the TM-PO bond. They correlated orbital interactions, bond lengths, population analysis, and atomic charges in order to achieve reasonable explanations about the observed trends on the vibrational frequencies of coordinated PO in comparison with NO and CO. The authors performed DFT calculations for various transition metal complexes, in which PO can assume different patterns of coordination, e.g. μ_3 and $\mu_4$coordination or as terminal ligand [38]. According to these authors, the orbital interactions between PO and transition metals occur predominantly via π backdonation, independent of the nature, coordination mode or oxidation state of the transition metal. They also observed that the properties of the TM–PO bonds such as bond length, bond strength and stretching vibrational frequencies are determined by the orbitals interactions and by electrostatic interactions as well.

As the number of theoretical papers devoted to investigate the nature of TM–PO and TM≡P bonding is scarce [38,40], we decided to carry out a comparative theoretical study of phosphorus and nitrogen complexes [Mo(P)$(NH_2)_3$] (**1**), [Mo(N)$(NH_2)_3$] (**2**), [Mo(PO)$(NH_2)_3$] (**3**), [Mo(NO)$(NH_2)_3$] (**4**), [Mo$(CO)_5$(PO)]$^+$ (**5**) and [Mo$(CO)_5$(NO)]$^+$ (**6**) (Fig. 1). The results of this work shed new light on the bonding situation of PO and its congener NO coordinated with Mo and they reveal the differences between Mo≡P and Mo≡N chemical bonds in phosphido **1** and nitrido **2** complexes. We report about the equilibrium geometries and the vibrational frequencies using DFT calculations at the BP86/TZ2P level. The electronic structure of the Mo–PO, Mo–NO, Mo–PO$^+$, Mo–NO$^+$, Mo≡P, and Mo≡N bonds was analyzed in terms of the donor–acceptor model of Dewar, Chatt, and Duncanson [41–44], employing the energy decomposition analysis. The topological analysis of the electron density, including the Laplacian distribution $\nabla^2\rho$(r) of **1–6** was also carried out [45,46]. Furthermore, the bond orders, atomic charges, atomic polarization coefficients, and hybridizations of complexes **1–6** were calculated with natural bond orbitals analysis [47].

2 Methods

The geometries, harmonic frequencies, and the bonding analysis have been calculated at the nonlocal DFT level of theory using the exchange functional of Becke [48] and the correlation functional of Perdew [49] (BP86). Uncontracted Slater-type orbitals (STOs) were used as basis functions for the SCF calculations [50]. Triple-ζ-quality basis sets were used which were augmented by two sets of polarization functions: p and d functions for the hydrogen atom and d and f functions for the other atoms. This level of theory is denoted as BP86/TZ2P. An auxiliary set of s, p, d, f, and g STOs were used to fit the molecular densities and represent the Coulomb and exchange potentials accurately in each SCF cycle [51]. Scalar relativistic effects have been considered for the transition metals using the zero-order regular approximation (ZORA) [52–54]. The calculations were performed using the ADF-(2006.1) program package [55,56]. All structures reported here have been checked to be energy minima on the potential energy surface.

The nature of Mo–PO, Mo–NO, Mo–PO$^+$, Mo–NO$^+$, Mo≡P, and Mo≡N chemical bonds was analyzed by means of NBO analysis [47], topological analysis of electron density [45,46], and the energy decomposition analysis (EDA), which is implemented in the program ADF and was originally developed by Morokuma [57,58] and by Ziegler and Rauk [59]. EDA has been proven to be a reliable and a powerful tool, improving the understanding about the nature of chemical bonding in main group compounds [60,61] and in transition-metal complexes [62,63]. Since this method has been discussed in detail in the current literature [62–64], we will describe the involved theory only briefly. The focus of the bonding analysis is the instantaneous interaction between the two fragments of the molecule, ΔE_{int}, which is the energy difference between the molecule and its fragments in the frozen geometry of the compound. ΔE_{int} can be decomposed

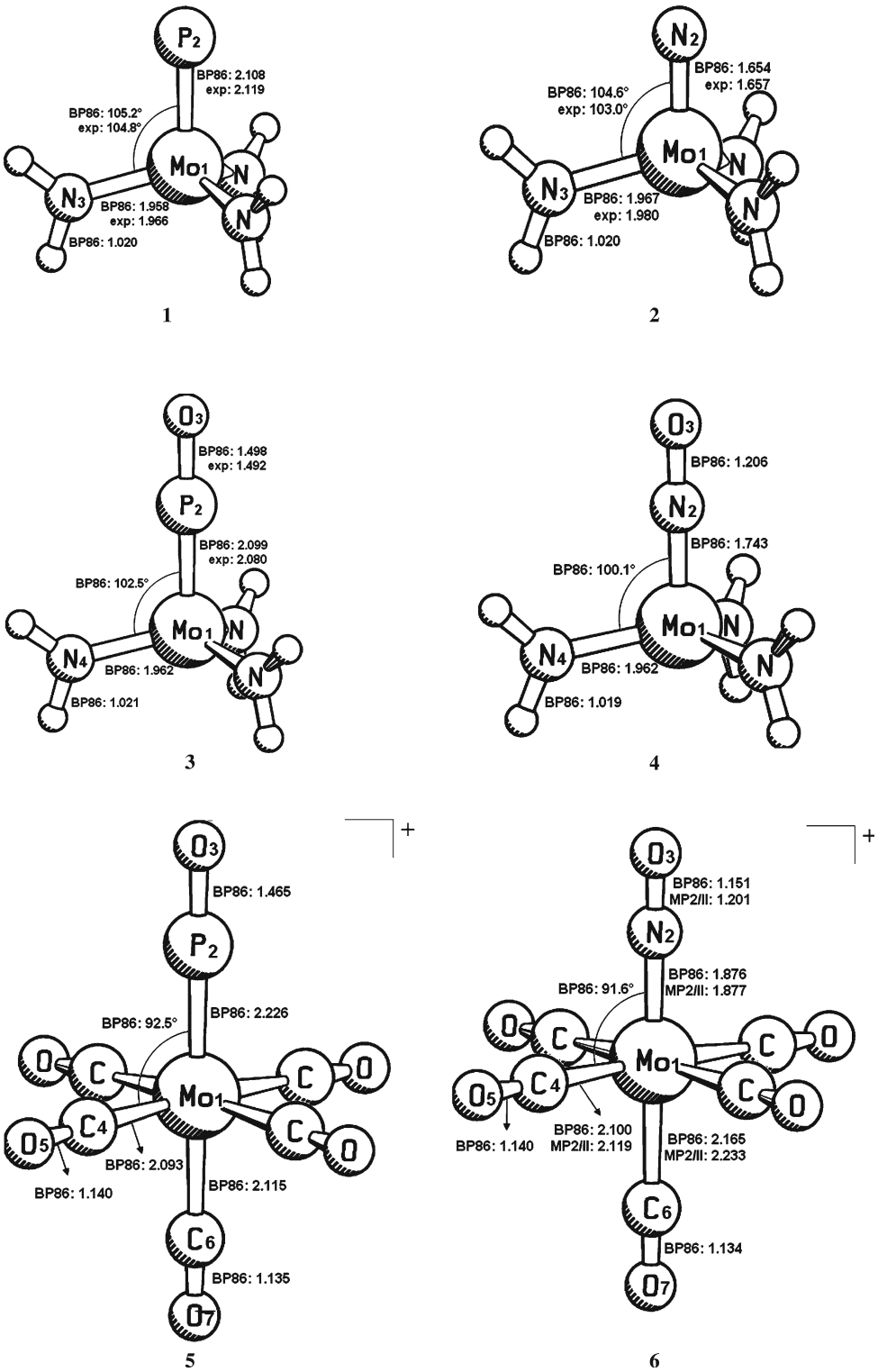

Fig. 1 Calculated (BP86/TZ2P) and experimental (see Refs [18,72,73]) geometries. For complex **6**, MP2/II values were taken from Ref. [74]. The bond distances are depicted in Å and the bond angles in degrees)

into three different components (Eq. 1),

$$\Delta E_{\text{int}} = \Delta E_{\text{elstat}} + \Delta E_{\text{Pauli}} + \Delta E_{\text{orb}} \quad (1)$$

where ΔE_{elstat} is the quasiclassical electrostatic interaction between the fragments and is calculated by considering the frozen electron-density distribution of the fragments in the geometry of the complex. The second term in Eq. 1, ΔE_{Pauli}, refers to the repulsive interactions between the fragments because two electrons with same spin cannot occupy the same region in space. It is obtained by enforcing the Kohn–Sham

determinant of the orbitals of the superimposed fragments to obey the Pauli principle by antisymmetrization and renormalization. In the last step of the EDA calculation, the third term of Eq. 1, ΔE_{orb}, is obtained by relaxing the molecular orbitals to their optimal forms in order to yield this stabilizing interaction. This term not only incorporates Heitler–London phenomenon [65] and has additional contribution of polarization and relaxation, but can also be partitioned into contributions from the orbitals belonging different irreducible representations of the point group of the interacting system. The interaction energy, ΔE_{int}, together with the term ΔE_{prep}, which is the energy necessary to promote the fragments from their equilibrium geometry and electronic ground state to the geometry and electronic state that they acquire in the ccompound, can be used to calculate the bond dissociation energy (Eq. 2). Further details about EDA can be found in the literature [55–64].

$$-D_{\mathrm{e}} = \Delta E_{\mathrm{prep}} + \Delta E_{\mathrm{int}}. \tag{2}$$

The figures of the molecular structures and orbitals presented in this manuscript and in the supporting information were obtained by using the ADFview program, available for the ADF-(2006.1) program package [55,56]. The Bader analysis [45,46] was carried out using AIMPAC suit of programs [66]. The NBO analysis [47] was performed by using the NBO 5.0 package [67], implemented in the Gaussian03 [68]. To perform NBO and AIM analyses, the effective core potential (ECP) MWB28 [69] was employed with the Gaussian basis set TZVP [70,71]. The latter calculations at BP86/TZVP were carried out using the geometries which were optimized at BP86/TZ2P.

3 Geometries and vibrational frequencies

Figure 1 shows the optimized geometries of the model compounds **1–6** at BP86/TZ2P. Experimental values of substituted derivatives of **1–3** [18,72,73] and calculated values of **6** from a previous study at the MP2/II level [74] are also shown. The calculated bond lengths of **1–3** are in good agreement with the experimental data and the BP86/TZ2P values concur with previous MP2/II values where the basis set has DZP quality [74].

The calculated and experimental distances for the $(NH_2)_3$Mo–PO bond in **3** are slightly shorter than for the $(NH_2)_3$Mo–P bond in **1** but the calculations predict that the $(NH_2)_3$Mo–NO bond in **4** should be clearly longer than the $(NH_2)_3$Mo–N bond in **2**. The Mo–PO and Mo–NO bonds in the formally Mo(VI) compounds **5** and **6** are significantly longer than in the formally Mo(0) compounds **3** and **4** while the P–O and N–O bonds in the latter species are clearly shorter than in the former complexes. The BP86/TZ2P calculations predict that the interatomic distances in free PO (1.476 Å) and NO (1.151 Å) which were calculated in the $X^2\Pi$ electronic ground state become longer in **3** and **4** while they are shorter in **5** or remain constant in **6**. The change in the P–O and N–O distances between the free species and the complexes agrees with the trend of the calculated stretching frequencies ν(PO) and ν(NO) . The theoretically predicted wavenumber for the harmonic modes of the free species are $\nu(\mathrm{PO}) = 1{,}233\,\mathrm{cm}^{-1}$ and $\nu(\mathrm{NO}) = 1{,}904\,\mathrm{cm}^{-1}$. The calculated frequencies for the molybdenum complexes are $\nu(NH_2)_3$Mo–PO $= 1{,}221\,\mathrm{cm}^{-1}$, $\nu(NH_2)_3$Mo–NO $= 1{,}669\,\mathrm{cm}^{-1}$, $\nu(CO)_5$Mo–PO $= 1{,}310\,\mathrm{cm}^{-1}$ and $\nu(CO)_5$ Mo–NO $= 1{,}862\,\mathrm{cm}^{-1}$.

4 Bonding analysis

The focus of our work is on the analysis of the metal–ligand bonding situation using charge- and energy decomposition methods. The results of the charge analyses are discussed first. Tables 1 and 2 give the NBO results for the complexes **1–6**.

The Wiberg bond orders [75] shown in Table 1 suggest that the $(NH_2)_3$Mo–P bond in **1** ($b_{AB}^{(w)} = 2.550$) and the terminal $(NH_2)_3$Mo–N bond in **2** ($b_{AB}^{(w)} = 2.640$) have triple bond character. Since the bonds are polar, the bond orders should have a value < 3. The bond polarization and hybridization of the NBOs given in Table 2 indicate that the σ and the degenerate π components of the Mo–P bond in **1** are slightly polarized toward the metal end while the σ and π components of the Mo–N bond in **2** are polarized toward nitrogen. The calculated charge distribution gives positive partial charges for Mo in both compounds **1** (+0.585 e) and **2** (+1.196 e). The latter value is much higher than the former because the molybdenum atom in $(NH_2)_3$MoN looses electronic charge to the terminal nitrogen atom which carries a negative charge of −0.380 e while the molybdenum atom in $(NH_2)_3$MoP gains electronic charge from the terminal phosphorus atom which has a positive charge of +0.136 e. Note that Mo and P atoms in **1** carry positive partial charges. The electrostatic contributions to the bond are frequently estimated using atomic partical charges which would mean that there is a repulsive electrostatic contribution to the Mo–P bond in **1**. The reasoning is not valid, because atomic partical charges are scalar quantities which do not give any information about the spatial distribution of the electronic charge. It will be shown below that the electrostatic contribution to the Mo–P bond in **1** is strongly attractive.

The calculated bond orders for the PO and NO complexes **3** and **4** suggest that the Mo–PO bond in **3** (1.941) and the Mo–NO bond in **4** (1.842) are closer to double bonds (Table 1). However, the NBO analysis gives three components for the Mo–PO bond in **3** and the Mo–NO bond in **4**, one σ and two degenerate π bonds (Table 2). The σ orbital

Table 1 Bond orders and atomic charges, obtained by NBO analysis for complexes **1**–**4**, at BP86/TZVP, ECP = MWB28

Compound	Bond	bond orders		Atomic charges	
		$b_{AB}^{(w)}$	$b_{AB}^{(nlmo/npa)}$	Atom/group	q^{NPA}
1	Mo(1)–P(2)	2.550	2.428	Mo(1)	0.585
	Mo(1)–N(3)	0.954	0.680	P(2)	0.136
				N(3)	−0.980
2	Mo(1)–N(2)	2.640	2.570	Mo(1)	1.196
	Mo(1)–N(3)	0.923	0.658	N(2)	−0.380
				N(3)	−1.018
3	Mo(1)–P(2)	1.941	1.770	Mo(1)	0.521
	Mo(1)–N(4)	0.932	0.670	P(2)	1.165
	P(2)–O(3)	1.440	0.950	O(3)	−0.861
				N(4)	−1.005
				P(2)–O(3)	0.304
4	Mo(1)–N(2)	1.842	1.950	Mo(1)	1.100
	Mo(1)–N(4)	0.915	0.650	N(2)	0.080
	N(2)–O(3)	1.609	1.296	O(3)	−0.301
				N(4)	−1.028
				N(2)–O(3)	−0.221
5	Mo(1)–P(2)	1.156	0.939	Mo(1)	−1.298
	Mo(1)–C(4)	0.697	0.694	P(2)	1.527
	Mo(1)–C(6)	0.631	0.633	O(3)	−0.716
	P(2)O(3)	1.738	1.182	C(4)	0.600
	C(4)O(5)	2.300	1.534	C(6)	0.639
	C(6)O(7)	2.357	1.431	O(5)	−0.320
				O(7)	−0.238
				P(2)–O(3)	0.811
6	Mo(1)–N(2)	1.280	0.911	Mo(1)	−0.727
	Mo(1)–C(4)	0.682	0.641	N(2)	0.320
	Mo(1)–C(6)	0.599	0.576	O(3)	−0.025
	N(2)O(3)	2.000	1.334	C(4)	0.590
	C(4)O(5)	2.318	1.418	C(6)	0.595
	C(6)O(7)	2.358	1.431	O(5)	−0.308
				O(7)	−0.292
				N(2)–O(3)	0.295

$b_{AB}^{(w)}$ Wiberg bond index, $b_{AB}^{(nlmo/npa)}$ Atom–atom net linear NLMO/NPA bond orders

is significantly polarized toward the P and N end, respectively, while the Mo–PO and Mo–NO π bonds in **3** and **4** are slightly more polarized toward the metal end compared with the Mo–P and Mo–N π bonds in **1** and **2**. The stronger polarization of the σ and π bonds in **3** and **4** explain why the triple bonds have smaller bond orders than the triple bonds in **1** and **2**. Partial double bond character is also suggested by the calculated bond orders for the P–O bond (1.440) in **3** and the N-O bond (1.609) in **4**. Since thee bonding components are assigned to the Mo–PO bond in **3** and the Mo–NO bond in **4**, there is only one σ component possible for the P–O and N–O bonds in the two compounds. The NBO calculations were carried out with allowance for three-center bonding but they did not give a π bonding contribution for the P–O and N–O bonds in **3** and **4**. We think that the NBO results should be interpreted such that the π contributions of the Mo–PO and Mo–NO bonds are larger than those of the P–O and N–O bonds, respectively. Although the total bond orders in **3** and **4** are even smaller than **2**, the bonds may be interpreted as triple bonds because there are one σ and two π bonds which explains that the Mo–PO bond length in **3** is even slightly shorter than in **1**. It will be shown below that the Mo–PO bond in **3** is also stronger than the Mo–P bond in **1**. The latter results should not be interpreted as a failure of the NBO method. Rather, they show that the description of chemical bonds in terms of a single Lewis structure is not adequate for delocalized systems, which is well known.

The charge analyses for **5** and **6** indicate that the Mo–P–O and Mo–N–O bonds in the low-valent Mo(0) complexes are very different from the bonds in the high-valent Mo(VI) compounds **3** and **4**. The bond orders shown in Table 1 for the Mo–PO bond in **5** (1.156) and the Mo–NO bond in **6** (1.280) are only slightly higher than for a single bond while the bond orders for the P–O bond (1.738) and the N–O bond (2.000) suggest double bond character. The interpretation is supported by the NBO results for **5** (Table 2) which now gives three components, one σ orbital and two degenerate π orbitals for the P–O bond while the Mo–PO bond has only one component with σ symmetry. The NBO results for **6** sketch a rather unusual bonding situation. The Mo–NO bond has two degenerate π contributions but no σ contribution while the N–O bond has only a σ orbital but no π orbitals. The result can be understood when one realized that the NBO algorithm, which is designated to give the most favorable Lewis structure, is critically challenged when it comes to transition metal complexes where the number of relevant bonding orbitals greatly exceeds the number of availabe electron pairs. There are three bonding contributions for each Mo–CO bond, one σ orbital for the Mo←CO donation and two degenerate π contributions for the Mo→CO backdonation. This yields 15 orbital contributions to the Mo-CO bonding in $[(CO)_5Mo(NO)]^+$ (**6**) which are difficult to cast into a Lewis picture.

The significant differences in the bonding situation between **3** and **4**, on the one hand side and **5** and **6**, on the other side comes also to the fore by the calculated particle charges (Table 1). The molybdenum atom in **3** and **4** carries a large positive charge but the Mo atom in **5** and **6** has a large negative charge. The PO and NO moieties in the latter low-valent complexes possess ~0.5 electrons less than in the high-valent compound **3** and **4**.

We analyzed the charge distribution in compounds **1**–**6** with AIM method (Atoms in Molecules) developed by Bader [45,46]. Figure 2 shows the contour line diagrams of the

Table 2 Atomic polarization coefficients, and hybridizations of the metal–ligand, P–O, and N–O bonds at BP86/TZVP, ECP = MWB28

		Polarization coefficients / hybridization							
Compound	Bond (M–L)	M%	L%	s% (M)	p% (M)	d% (M)	s% (L)	p% (L)	d% (L)
1	Mo(1)–P(2)$_\sigma$	52.1	47.0	15.6	0.4	84.0	12.2	87.3	0.5
	Mo(1)–P(2)$_\pi$	55.3	42.5	0.0	0.1	99.9	0.0	99.6	0.4
	Mo(1)–P(2)$_\pi$	55.4	42.4	0.0	0.1	99.9	0.0	99.6	0.4
	Mo(1)–N(3)	24.1	75.3	13.5	0.2	86.3	41.8	58.2	0.0
2	Mo(1)–N(2)$_\sigma$	41.5	57.4	5.0	0.1	94.9	17.6	82.2	0.1
	Mo(1)–N(2)$_\pi$	46.7	52.1	0.0	0.1	99.9	0.0	99.9	0.1
	Mo(1)–N(2)$_\pi$	46.7	52.1	0.0	0.1	99.9	0.0	99.9	0.1
	Mo(1)–N(3)	23.0	76.5	14.9	0.2	84.9	40.6	59.4	0.0
3	Mo(1)–P(2)$_\sigma$	29.0	69.9	22.5	0.1	77.4	74.5	25.5	0.0
	Mo(1)–P(2)$_\pi$	65.3	32.1	0.0	0.3	99.7	0.0	99.0	1.0
	Mo(1)–P(2)$_\pi$	65.3	32.1	0.0	0.3	99.7	0.0	99.0	1.0
	Mo(1)–N(4)	24.1	75.4	11.7	0.2	88.2	41.7	58.3	0.0
	P(2)–O(3)	28.7	71.0	47.1	52.5	0.4	27.4	72.5	0.2
4	Mo(1)–N(2)$_\sigma$	23.1	76.4	15.7	0.1	84.2	65.3	34.7	0.0
	Mo(1)–N(2)$_\pi$	49.8	48.8	0.0	0.1	99.9	0.0	100.0	0.0
	Mo(1)–N(2)$_\pi$	49.8	48.8	0.0	0.0	99.9	0.0	100.0	0.0
	Mo(1)–N(4)	23.6	76.0	13.7	0.2	86.2	40.6	59.4	0.0
	N(2)–O(3)	46.1	53.8	40.5	59.4	0.1	26.8	73.0	0.2
5	Mo(1)–P(2)	31.2	68.9	35.9	0.1	64.0	63.9	36.1	0.0
	Mo(1)–C(4)	31.3	68.8	29.3	0.1	70.7	64.4	35.6	0.0
	Mo(1)–C(6)	31.3	68.8	29.3	0.1	70.7	64.4	35.6	0.0
	P(2)–O(3)$_\sigma$	26.5	73.5	38.1	61.4	0.5	29.3	70.5	0.2
	P(2)–O(3)$_\pi$	21.9	78.1	0.0	97.0	3.0	0.0	99.8	0.2
	P(2)–O(3)$_\pi$	21.9	78.1	0.0	97.0	3.0	0.0	99.8	0.2
6	Mo(1)–N(2)$_\pi$	59.0	41.0	0.3	0.0	99.7	0.0	100.0	0.0
	Mo(1)–N(2)$_\pi$	59.0	41.0	0.3	0.0	99.7	0.0	100.0	0.0
	Mo(1)–C(4)	29.1	70.9	34.6	0.1	65.3	64.2	35.8	0.0
	Mo(1)–C(6)	25.0	75.1	30.1	0.1	69.8	64.8	35.2	0.0
	N(2)–O(3)	43.9	56.1	39.0	60.8	0.2	31.5	68.3	0.2

Laplacian $\nabla^2\rho(r)$ in the plane of the molecules which contains the Mo–X (X = N, P, NO, PO) moieties. The shape of the Laplacian in the vicinity of the terminal Mo–P and Mo–N bonds of **1** and **2** exhibits a circular form at Mo and N while the phosphorus atom has a somewhat distorted shape with an area of charge concentration ($\nabla^2\rho$(r) < 0, solid lines) pointing toward Mo. The latter distortion becomes much larger in the Mo–PO moiety of **3** (Fig. 2c) where two areas of charge concentration at P atom are found in the π bonding region. A slight distortion towards a squarish shape is also exhibited at the Mo atom of **3** as well as **4**. Note that the NO bond in **4** has a continuous area of charge concentration while the PO bond in **3** possesses an area of charge concentration at oxygen but there is charge depletion ($\nabla^2\rho\,(r) > 0$, dashed lines) at the phosphorus end. The shape of the Laplacian indicates that the N–O bond in **4** is more covalent than the P–O bond in **3** and that both bonds are more covalent than the Mo–PO and Mo–NO bonds. It is interesting to see that the Laplacian for the Mo–PO and Mo–NO bonds in the low-valent complexes **5** and **6** have nearly the same shape as in the high-valent complexes **3** and **4**. This shows that the visual inspection of the Laplacian is not very sensitive to explore the differences between the bonding situation of related compounds.

More quantitative information about the AIM analysis comes from the numerical data which are given in Table 3. According to Bader [45,46], an electron-sharing (covalent) bond is characterized by a negative value of the Laplacian at the bond critical point $\nabla^2\rho_b$ while closed-shell interactions (ionic bonds and van der Waals bonds) have positive values of $\nabla^2\rho_b$. The calculated data in Table 3 would then suggest that all bonds which were analyzed by us with the AIM are ionic except for the Mo–P bond in **1** and the N–O bonds in **4** and **6**. This is a suprising finding particularly for the C-O bonds because the shape of the Laplacian shows a

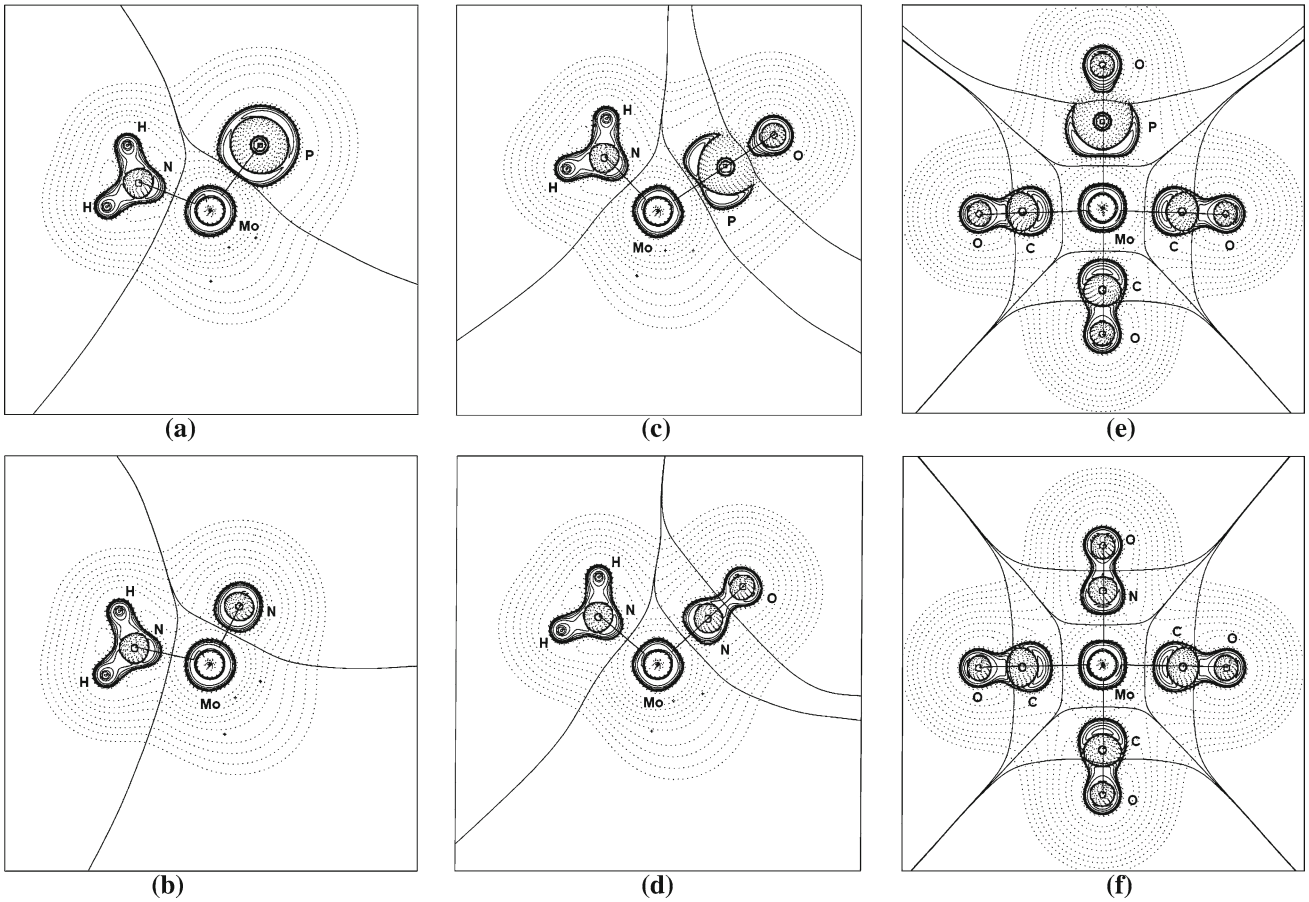

Fig. 2 Contour-line diagrams of the Laplacian distribution $\nabla^2\rho$(r) of (a) **1** and (b) **2** in the Mo(1)P(2)N(4) plane at BP86/TZVP. *Dashed lines* indicate local charge depletion ($\nabla^2\rho_b > 0$) and *solid lines* indicate local charge concentration ($\nabla^2\rho_b < 0$). The *solid lines* connecting the atomic nuclei are the bond paths and the *solid lines* separating the atomic nuclei indicate the zero-flux surfaces in the molecular plane. The crossing points of the bond paths and zero-flux surfaces are the bond critical points (BCPs). Contour-line diagrams of the Laplacian distribution $\nabla^2\rho(r)$ of (a) **3** and (b) **4** in the Mo(1)N(2)N(4) plane, obtained at BP86/TZVP. Contour-line diagrams of the Laplacian distribution $\nabla^2\rho(r)$ of (a) **5** (b) and **6** in the molecular plane containing atoms 1–7, obtained at BP86/TZVP

continuous area of charge concentration between the carbon and oxygen atom (Figs. 2e, f). It was already pointed out by Cremer and Kraka [76] that the value of the Laplacian is not a very reliable indicator for a covalent bond. They suggested that the energy density at the bond critical point H_b is a better criterion. A negative value for H_b indicates an electron-sharing (covalent) bond while a positive or zero value of H_b suggests closed-shell interactions (ionic bonds and van der Waals bonds). Table 3 shows that the H_b values are negative for all bonds and that the C–O bonds in **5** and **6** possess particularly large negative H_b values. Note that the terminal Mo–X (X = N, P, NO, PO) bonds have only small negative H_b values which suggests that these bond have a large ionic character. The latter result is not in agreement, however, with the triple bonds which are found by the NBO analysis for the terminal Mo–P, Mo–N, Mo–PO and Mo–NO bonds of **1**–**4**.

We also analyzed the nature of the terminal Mo–P, Mo–N, Mo–PO and Mo–NO bonds of **1**–**6** with the EDA method. The numerical results for **1**–**4** are shown in Table 4. A crucial factor for the EDA is the choice of the interacting fragments which was straightforward for the Mo–P and Mo–N bonds of **1** and **2**. The electronic ground states of the fragments $(NH_2)_3Mo$ and X (X = P, O) is a quartet state where the unpaired electrons are in σ and degenerate π orbitals as schematically shown in Scheme 1a. The choice of the electronic states for the fragments of **3** and **4** is less obvious. The ligands PO and NO have a doublet ground state while the metal fragments are quartets. Test calculations showed that the interactions where both fragments are in a doublet state are better suited to describe the bonding situation in the compounds than choosing fragments in the quartet state. Scheme 1b schematically shows the occupation of the interacting fragments in the doublet state which yield the molecule in the singlet state. There is one Mo←XO (X = P, O) σ-donor orbital, one Mo→XO π orbital for the backdonation and one Mo–XO electron-sharing orbital. The

Table 3 Bond critical points properties (a.u.) and calculated bond distances r(Å) of complexes **1–6** at BP86/TZVP

Molecules	BCPs	ρ_b	$\nabla^2\rho_b$	ε	H_b	r
1	Mo(1)–P(2)	0.148	−0.056	0.000	−0.103	2.108
	Mo(1)–N(3)	0.137	0.437	0.158	−0.048	1.958
2	Mo(1)–N(2)	0.299	0.534	0.000	−0.248	1.654
	Mo(1)–N(3)	0.135	0.434	0.160	−0.045	1.967
3	Mo(1)–P(2)	0.114	0.286	0.000	−0.054	2.099
	Mo(1)–N(4)	0.137	0.439	0.081	−0.045	1.962
	P(2)–O(3)	0.208	1.353	0.000	−0.129	1.498
4	Mo(1)–N(2)	0.196	1.001	0.000	−0.092	1.743
	Mo(1)–N(4)	0.135	0.443	0.041	−0.045	1.962
	N(2)–O(3)	0.502	−1.175	0.000	−0.690	1.206
5	Mo(1)–P(2)	0.087	0.282	0.000	−0.028	2.227
	Mo(1)–C(4)	0.097	0.360	0.190	−0.024	2.093
	Mo(1)–C(6)	0.093	0.327	0.000	−0.022	2.115
	C(4)–O(5)	0.475	0.831	0.003	−0.833	1.140
	C(6)–O(7)	0.481	0.900	0.000	−0.846	1.135
	P(2)–O(3)	0.224	1.670	0.000	−0.136	1.465
6	Mo(1)–N(2)	0.137	0.806	0.000	−0.036	1.876
	Mo(1)–C(4)	0.095	0.359	0.218	−0.023	2.100
	Mo(1)–C(6)	0.082	0.315	0.000	−0.015	2.165
	C(4)–O(5)	0.476	0.841	0.001	−0.834	1.140
	C(6)–O(7)	0.482	0.909	0.000	−0.848	1.134
	N(2)–O(3)	0.585	−1.745	0.000	−0.965	1.151

All values are in a.u. One atomic unit of $\rho_b = 6.748\,e\text{Å}^{-3}$, of $\nabla^2\rho_b = 24.10\,e\text{Å}^{-5}$, and of energy = $e2/a0 = 627.51$ kcal/mol = 27.21 eV

EDA method makes it possible to treat the π components of the Mo–XO bond equally using fractional occupation numbers. For the EDA calculations of **3** and **4**, the degenerate antibonding π^* orbitals of XO are occupied with 0.5 electrons each, while the degenerate d(π) orbitals of the metal are occupied with 1.5 electrons. This gives a balanced description of the π interactions for the Mo–XO bonds in **3** and **4**.

The EDA data in Table 3 show that the Mo–N bond of **1** is much stronger ($\Delta E_{int} = -175.7$ kcal/mol) than the Mo–P bond of **2** ($\Delta E_{int} = -118.6$ kcal/mol). Both bonds have a larger orbital (covalent) contribution than electrostatic contribution which is revealed by the percentage values of the ΔE_{orb} and ΔE_{elstat} terms. It is interesting to note that the σ and π bonding interactions to the Mo–P and Mo–N bonds have nearly equal strength. This is in agreement with the NBO results (Table 2) which suggest that the σ and π orbitals are both not very polarized toward either end. The preparation energies of the metal fragment $\Delta E_{prep(f1)}$ are not very large and hence, the bond dissociation energies D_e of the Mo–P and Mo–N bonds of **1** (105.0 kcal/mol) and **2** (162.1 kcal/mol) are only slightly smaller than the ΔE_{int} values.

The EDA data suggest that the Mo–PO bond in **3** is stronger than the Mo–P bond in **1** while the Mo–NO bond in **4** is weaker than the Mo–N bond in **2**. This is in agreement with the trend of the bond lengths (Fig. 1) but it must be mentioned that bond length and bond energy do not necessarily correlate with each other (For pertinent examples see [77,78]). The EDA data suggest that there are significant differences between the Mo–PO and Mo–NO bonds in **3** and **4**

Table 4 EDA of Mo–P, Mo–N, Mo–PO, and Mo–NO bonds of complexes **1–4** at BP86/TZ2P

	1	2	3	4
(f1)	$[Mo(NH_2)_3]$	$[Mo(NH_2)_3]$	$[Mo(NH_2)_3]$	$[Mo(NH_2)_3]$
(f2)	P	N	PO	NO
symmetry	C_{3v}	C_{3v}	C_{3v}	C_{3v}
ΔE_{int}	−118.6	−175.7	−129.0	−154.2
ΔE_{pauli}	283.2	437.0	157.1	222.6
ΔE_{elstat}	−201.7 (43.8%)[a]	−236.5 (38.6%)	−62.9 (21.2%)	−92.8 (24.6%)
ΔE_{orb}	−200.1 (56.2%)	−376.2 (61.4%)	−223.2 (78.8%)	−284.0 (75.4%)
$\Delta E_{(A1)}$	−97.1	−192.8	−42.9	−53.2
$\Delta E_{(A2)}$	0.0	0.0	0.0	0.0
$\Delta E_{(E1)}$	−103.1	−183.4	−180.3	−230.8
ΔE_σ	−97.1 (48.5%)[b]	−192.8 (51.2%)	−42.9 (19.2%)	−53.2 (18.7%)
ΔE_π	−103.1 (51.5%)	−183.4 (48.8%)	−180.3 (80.8%)	−230.8 (81.3%)
$-D_e$	−105.0	−162.1	−111.6	−134.8
$\Delta E_{prep(f1)}$	13.6	13.5	22.8	20.7
$\Delta E_{prep(f2)}$	0.0	0.0	5.4	9.6
$\Delta E_{exc(f2)}$	–	–	–	–

Energy contributions in kcal mol^{-1}

[a] Values in parentheses give the percentage of attractive interactions $\Delta E_{elstat} + \Delta E_{orb}$

[b] The value in parentheses gives the percentage contribution to the total orbital interactions, ΔE_{orb}

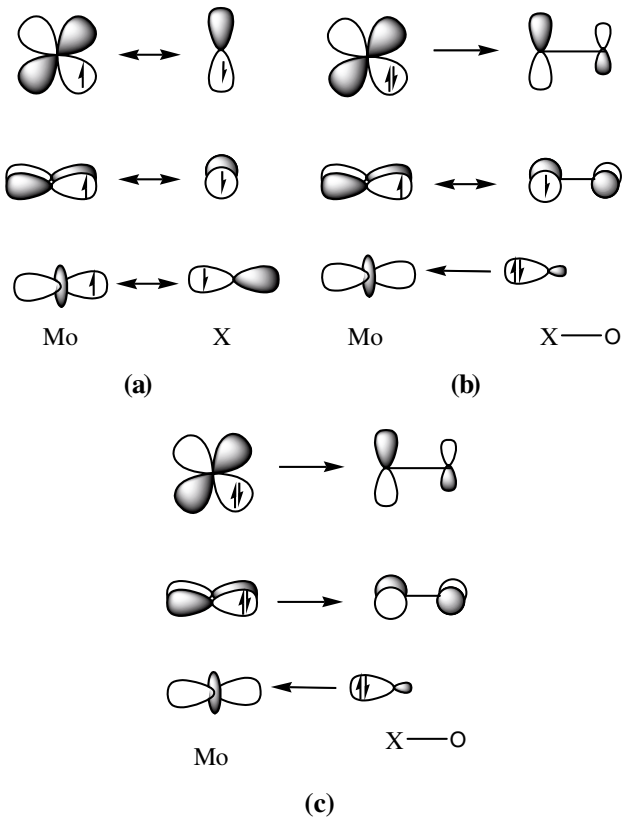

Scheme 1 Schematic representation of the electronic structures of the interacting fragments which are chosen for the EDA. **a** Interacting fragments of complexes **1** and **2** in the quartet states, X = P, N. **b** Interacting fragments of complexes **3** and **4** in the dublet states, X = P, N. Note that in the EDA calculations the d(π) orbitals of the metal are occupied with 1.5 electrons (*top*) and 0.5 electrons (*center*) and that the π orbitals of XO are occupied with 0.5 electrons each. **c** Interacting fragments of complexes **5** and **6** where X-O is PO^+, NO^+ or CO

on the one hand side and the Mo–P and Mo–N bonds in **1** and **2**, on the other hand. The former bonds have a much larger covalent character than the latter bonds which is suggested by the higher percentage contribution of the ΔE_{orb} term which contributes between 75 and 79% to the total interaction energy (Table 4). The orbital contributions to the Mo–PO and Mo–NO bonds in **3** and **4** have also a much larger π character which attains ~80% of the total ΔE_{orb} term. This is in agreement with the NBO results (Table 2) which indicate that the Mo–PO and Mo–NO σ bonds are much more polarized than the π bonds.

The EDA results for the positively charged complexes **5** and **6** are shown in Table 5. The results for the Mo–PO^+ and Mo–NO^+ bonds in **5** and **6** are not directly comparable with the data for **3** and **4** because the interacting fragments in the former compounds are closed-shell species $(CO)_5Mo$ and XO^+ (X = P, N) where the bonding can be interpreted using the Dewar–Chatt–Duncanson model [41–44] (See Scheme 1c), while in **3** and **4** neutral open–shell species have been chosen. We also analyzed the metal-CO bonding in **5** and **6** and compared it with the Mo–PO^+ and Mo–NO^+ bonds because they are valence isoelectronic. The EDA data indicate that there is no attractive contribution from the ΔE_{elstat} term to the Mo–PO^+ and Mo–NO^+ bonds and that the binding interactions solely come from the orbital term ΔE_{orb}. The calculated interaction energies and bond dissociation energies predict that the Mo–PO^+ and Mo–NO^+ bonds in **5** and **6** are clearly weaker than the Mo–PO and Mo–NO bonds in **3** and **4** (Table 5). For all systems **3** - **6** holds that the π interactions are much more important than the σ bonding. The results for the Mo–PO^+ and Mo–NO^+ bonds in **5** and **6** are quite different to the nature of the Mo–CO bonds. The latter bonds have only ~50% covalent character and the contribution of the σ orbitals to the ΔE_{orb} term has about the same strength as the contribution of the π orbitals.

5 Summary and conclusions

The calculated results which are reported in this work give a comprehensive description of the metal–ligand bonding situation in the molybdenum compounds **1**–**6**. The NBO and EDA data complement each other in the interpretation of the interatomic interactions while the numerical AIM results must be interpreted with caution. The terminal $(NH_2)_3Mo$–P and $(NH_2)_3Mo$–N bonds in **1** and **2** are clearly electron-sharing triple bonds. The terminal $(NH_2)_3Mo$–PO and $(NH_2)_3Mo$–NO bonds in **3** and **4** have also three bonding contributions from a σ and a degenerate π orbital where the σ components are more polarized toward the ligand end and the π orbitals are more polarized toward the metal end than in **1** and **2**. The EDA calculations show that the π bonding contributions to the $(NH_2)_3Mo$–PO and $(NH_2)_3Mo$–NO bonds are much more important than the σ contributions while σ and π bonding have nearly equal strength in the terminal $(NH_2)_3Mo$–P and $(NH_2)_3Mo$–N bonds in **1** and **2**. The total $(NH_2)_3Mo$–PO binding interaction is stronger than for $(NH_2)_3Mo$–P which is in agreement with the shorter Mo–PO bond compared with the Mo–P bond. The calculated bond orders suggest that there are only $(NH_2)_3Mo$–PO and $(NH_2)_3Mo$–NO double bonds which comes from the larger polarization of the σ and π contributions but a closer inspection of the bonding shows that these bonds should also be considered as electron-sharing triple bonds. The bonding situation in the positively charges complexes $[(CO)_5Mo$–$(PO)]^+$ and $[(CO)_5Mo$–$(NO)]^+$ is best described in terms of $(CO)_5Mo \rightarrow XO^+$ donation and $(CO)_5Mo \leftarrow XO^+$ backdonation (X = P, N) using the familiar Dewar–Chatt–Duncanson model. The latter bonding interactions are stronger and have a larger π character than the Mo–CO bonds.

Table 5 EDA of Mo–NO^+, Mo–PO^+, Mo-$CO_{(ax)}$, and Mo-$CO_{(eq)}$ bonds of complexes **5** and **6** at BP86/TZ2P[a]

	5			6		
(f1)	$[Mo(CO)_5]$	$[Mo(CO)_4PO]^+$	$[Mo(CO)_4PO]^+$	$[Mo(CO)_5]$	$[Mo(CO)_4NO]^+$	$[Mo(CO)_4NO]^+$
(f2)	PO^+	$CO_{(ax)}$	$CO_{(eq)}$	NO^+	$CO_{(ax)}$	$CO_{(eq)}$
symmetry	C_{4v}	C_{4v}	C_s	C_{4v}	C_{4v}	C_s
ΔE_{int}	−76.8	−38.8	−42.6	−121.9	−34.7	−40.4
ΔE_{pauli}	78.2	87.0	92.9	103.4	71.6	89.6
ΔE_{elstat}	8.5	−64.4 (51.2%)	−69.9 (51.6%)	7.5	−55.0 (52.2%)[a]	−67.1 (51.6%)
ΔE_{orb}	−163.5	−61.4 (48.8%)	−65.6 (48.4%)	−232.8	−51.3 (47.8%)	−62.9 (48.4%)
$\Delta E_{(A')}$	–	–	−49.2	–	–	−46.8
$\Delta E_{(A'')}$	–	–	−16.5	–	–	−16.1
$\Delta E_{(A1)}$	−28.3	−37.2	–	−27.0	−30.7	–
$\Delta E_{(A2)}$	−0.4	0.0	–	−0.3	0.0	–
$\Delta E_{(B1)}$	−1.5	−0.1	–	−0.9	−0.1	–
$\Delta E_{(B2)}$	−3.1	−0.1	–	−2.1	−0.1	–
$\Delta E_{(E1)}$	−130.2	−24.0	–	−202.6	−20.5	–
ΔE_{σ}	−28.3 (17.3%)	−37.2 (60.6%)	−32.6 (49.7%)	−27.0 (11.6%)[b]	−30.7 (59.8%)	−30.7 (48.8%)
ΔE_{π}	−133.3 (82.7%)	−24.1 (39.4%)	−33.0 (50.3%)	−204.7 (88.4%)	−20.6 (40.2%)	−32.2 (51.2%)
$-D_e$	−67.1	−37.5	−38.9	−100.2	−33.0	−37.6
ΔE_{prep}	9.7	1.3	3.7	21.7	1.7	2.8

Energy contributions in kcal mol^{-1}

[a] Values in parentheses give the percentage of attractive interactions $\Delta E_{elstat} + \Delta E_{orb}$

[b] The values in parentheses give the percentage contribution to the total orbital interactions, ΔE_{orb}

Acknowledgments This work was supported by the Deutsche Forschungsgemeinschaft. The authors thank the computer center at HRZ Marburg for the excellent service and computational time provided. G. F Caramori thanks the Conselho Nacional de Desenvolvimento Científico e Tecnológico, CNPq—Brasil, for a post-doctoral scholarship (grant: 200786/2006–7).

References

1. Verma RD (1972) Can J Phys 50:1579
2. Verma RD (1973) Can J Phys 51:322
3. Prudhomme JC, Coquart B (1974) Can J Phys 52:2150
4. Haraguchi H, Fowler WK, Johnson DJ, Winefordner JD (1976) Spectrochem Acta Part A 32A:1539
5. Dyke JM, Morris A, Ridha A (1982) J Chem Soc Faraday Trans 2(78):207
6. Kawaguchi K, Saito S, Hirota E (1983) J Chem Phys 79:629
7. Kanata H, Yamamoto S, Saito S (1988) J Mol Spectrosc 131:89
8. Robertson EG, McNaughton D (2003) J Phys Chem A 107:642
9. Midda S, Das AK (2004) Int J Quantum Chem 98:447
10. Turner BE (1991) Astrophys J 376:573
11. Atalla RM, Singh PD (1987) Astrophys Space Sci 133:267
12. Matthews HE, Feldman PA, Bernath PF (1987) Astrophys J 312:358
13. Davies JE, Klunduk MC, Mays MJ, Raithby PR, Shields GP, Tompkin PK (1997) J Chem Soc Dalton Trans 715
14. Scherer OJ, Weigel S, Wolmershäuser G (1999) Heteroat Chem 10:622
15. Scherer OJ, Weigel S, Wolmershäuser G (1999) Angew Chem Int Ed 38:3688
16. Corrigan JF, Doherty S, Taylor NJ, Carty AJ (1994) J Am Chem Soc 116:9799
17. Wang W, Corrigan JF, Doherty S, Enright GD, Taylor NJ, Carty AJ (1996) Organometallics 15:2770
18. Johnson MJA, Odom AL, Cummins CC (1997) Chem Commun 1523
19. Yamamoto JH, Udachin KA, Enright GD, Carty AJ (1998) Chem Comm 2259
20. Yamamoto JH, Scoles L, Udachin KA, Enright GD, Carty AJ (2000) J Organomet Chem 600:84
21. Scoles L, Yamamoto JH, Brissieux L, Sterenberg BT, Udachin KA, Carty AJ (2001) Inorg Chem 40:6731
22. Tfouni E, Krieger M, McGarvey BR, Franco DW (2003) Coord Chem Rev 236:57 (and references therein)
23. Ford PC, Lorkovic IM (2002) Chem Rev 102:993
24. Wang PG, Xian M, Tang X, Wu X, Wen Z, Cai T, Janczuk A (2002) Chem Rev 102:1091
25. Lorkovic IM, Miranda KM, Lee B, Bernhard S, Schoonover JR, Ford PC (1998) J Am Chem Soc 120:11674
26. Borges SSS, Davanzo CU, Castellano EE, Z-Schpector J, Silva SC, Franco DW (1998) Inorg Chem 37:2670
27. Thiemens MW, Trogler WC (1991) Science 251:932
28. Laplaza CE, Odom AL, Davis WM, Cummins CC (1995) J Am Chem Soc 117:4999
29. Maxwell LR, Hendricks SB, Deming LS (1937) J Chem Phys 5:626
30. Hampson GC, Stosick AJ (1938) J Am Chem Soc 60:1814
31. Scherer OJ, Braun J, Walther P, Heckmann G, Wolmershäuser G (1991) Angew Chem Int Ed Engl 30:852
32. Lohr LL (1984) J Phys Chem 88:5569
33. Butler K, Kawaguchi EH (1983) J Mol Spectrosc 101:161
34. Andrews L, McCluskey M, Mielke Z, Withnall R (1990) J Mol Struct 222:95 (and references therein)

35. Hermann AW (1991) Angew Chem Int Ed Engl 30:818
36. Laplaza CE, Davis WM, Cummins CC (1995) Angew Chem Int Ed Engl 34:2042
37. Zanetti NC, Schrock RR, Davis WM (1995) Angew Chem Int Ed Engl 34:2044
38. Bérces A, Koentjoro O, Sterenberg BT, Yamamoto JH, Tse J, Carty AJ (2000) Organometallics 19:4336
39. Foerstner J, Olbrich F, Butenschon H (1996) Angew Chem Int Ed Engl 35:1234
40. Wagener T, Frenking G (1998) Inorg Chem 37:1805
41. Dewar MJS (1951) Bull Soc Chim Fr 18:C79
42. Chatt J, Duncanson LA (1953) J Chem Soc 2929
43. Frenking G (2001) J Organomet Chem 635:9
44. Frenking G (2002) In: Leigh GJ, Winterton N (eds) Modern coordination chemistry: the legacy of Joseph Chatt, The Royal Society, London, p 111
45. Bader RFW (1991) Chem Rev 91:893
46. Bader RFW (1990) Atoms in molecules. Claredon Press, Oxford
47. Reed AE, Weinhold F (1983) J Chem Phys 78:4066
48. Becke AD (1988) Phys Rev A 38:3098
49. Perdew JP (1986) Phys Rev B 33:8822
50. Snijders JG, Baerends EJ, Vernooijs P (1982) At Nucl Data Tables 26:483
51. Krijn J, Baerends EJ (1984) Fit functions in the HFS method, internal report (in Dutch), Vrije Universiteit, Amsterdam
52. van Lenthe E, Baerends EJ, Snijders JG (1993) J Chem Phys 99:4597
53. van Lenthe E, Baerends EJ, Snijders JG (1996) J Chem Phys 105:6505
54. van Lenthe E, van Leeuwen R, Baerends EJ, Snijders JG (1996) Int J Quantum Chem 57:281
55. Bickelhaupt FM, Baerends EJ (2000) Rev Comput Chem 15:1
56. te Velde G, Bickelhaupt FM, Baerends EJ, van Gisbergen SJA, Fonseca Guerra C, Snijders JG, Ziegler T (2001) J Comput Chem 22:931
57. Morokuma K (1971) J Chem Phys 55:1236
58. Morokuma K (1977) Acc Chem Res 10:294
59. Ziegler T, Rauk A (1977) Theor Chim Acta 46:1
60. Esterhuysen C, Frenking G (2004) Theor Chem Acc 111:81
61. Kovács A, Esterhuysen C, Frenking G (2005) Chem Eur J 11:1813
62. Frenking G, Wichmann K, Fröhlich N, Loschen C, Lein M, Frunzke J, Rayón VM (2003) Coord Chem Rev 55:238–239
63. Frenking G, Fröhlich N (2000) Chem Rev 100:717
64. Lein M, Frenking G (2005) In: Dykstra CE, Frenking G, Kim KS, Scuseria GE (eds) Theory and applications of computational chemistry: the first 40 years, Elsevier, Amsterdam p 291
65. Heitler W, London F (1927) Z Phys 44:455
66. Bader RFW (1995) AIMPAC—Source code obtained from the AIMPAC site at http://www.chemistry.mcmaster.ca/aimpac/aimpac.html McMaster University, Hamilton
67. Glendening ED, Badenhoop JK, Reed AE, Carpenter JE, Bohmann JA, Morales CM, Weinhold F (2001) NBO 5.0. Theoretical Chemistry Institute, University of Wisconsin, Madison
68. Frisch MJ, Trucks GW, Schlegel HB, Scuseria GE, Robb MA, Cheeseman JR, Montgomery JA Jr, Vreven T, Kudin KN, Burant JC, Millam JM, Iyengar SS, Tomasi J, Barone V, Mennucci B, Cossi M, Scalmani G, Rega N, Petersson GA, Nakatsuji H, Hada M, Ehara M, Toyota K, Fukuda R, Hasegawa J, Ishida M, Nakajima T, Honda Y, Kitao O, Nakai H, Klene M, Li X, Knox JE, Hratchian HP, Cross JB, Bakken V, Adamo C, Jaramillo J, Gomperts R, Stratmann RE, Yazyev O, Austin AJ, Cammi R, Pomelli C, Ochterski JW, Ayala PY, Morokuma K, Voth GA, Salvador P, Dannenberg JJ, Zakrzewski VG, Dapprich S, Daniels AD, Strain MC, Farkas O, Malick DK, Rabuck AD, Raghavachari K, Foresman JB, Ortiz JV, Cui Q, Baboul AG, Clifford S, Cioslowski J, Stefanov BB, Liu G, Liashenko A, Piskorz P, Komaromi I, Martin RL, Fox DJ, Keith T, Al-Laham MA, Peng CY, Nanayakkara A, Challacombe M, Gill PMW, Johnson B, Chen W, Wong MW, Gonzalez C, Pople JA (2004) Gaussian 03, Revision C.02, Gaussian, Wallingford
69. Andrae D, Haeussermann U, Dolg M, Stoll H, Preuss H (1990) Theor Chim Acta 77:123
70. Schaefer A, Horn H, Ahlrichs R (1992) J Chem Phys 97:2571
71. Schaefer A, Huber C, Ahlrichs R (1994) J Chem Phys 100:5829
72. Laplaza CE, Johnson MJA, Peters JC, Odom AL, Kim E, Cummins CC, George GN, Pickering IJ (1996) J Am Chem Soc 118:8623
73. Figueroa JS, Piro NA, Clough CR, Cummins CC (2006) J Am Chem Soc 128:940
74. Ehlers AW, Dapprich S, Vyboishchikov SF, Frenking G (1996) Organometallics 15:105
75. Wiberg K (1968) Tetrahedron 24:1083
76. Cremer D, Kraka E (1984) Angew Chem Int Ed Engl 23:627
77. Frenking G, Wichmann K, Fröhlich N, Grobe J, Golla W, Le Van D, Krebs B, Läge M (2002) Organometallics 21:2921
78. Fischer RA, Schulte MM, Weiß J, Zsolnai L, Jacobi A, Huttner G, Frenking G, Boehme C, Vyboishchikov SF (1998) J Am Chem Soc 120:1237